Proceedings of the IASS Annual Symposium 2023
Integration of Design and Fabrication
10 – 14 July 2023, Melbourne, Australia
Y.M. Xie, J. Burry, T.U. Lee and J. Ma (eds.)

# **Bio-based Composite Spatial Shell Structures**

Mostafa AKBARI\*,<sup>a</sup>, Farzaneh OGHAZIAN\*,<sup>c</sup>, Ji Yoon BAE<sup>d</sup>, Felecia DAVIS<sup>c</sup>, Laia MOGAS-SOLDEVILA<sup>d</sup> Masoud AKBARZADEH<sup>a,b</sup>

<sup>a</sup> Polyhedral Structures Laboratory, Weitzman School of Design, University of Pennsylvania, Philadelphia, USA Pennovation Center, 3401 Grays Ferry Ave. Philadelphia, PA, 19146

<sup>b</sup>General Robotic, Automation, Sensing and Perception (GRASP) Lab, School of Engineering and Applied Science, University of Pennsylvania, Philadelphia, USA

<sup>c</sup>Computational Textile Lab, College of Arts and Architecture, Penn State University, PA, 16801, USA

<sup>d</sup>DumoLab Research, Department of Architecture, Weitzman School of Design, University of Pennsylvania, Philadelphia, PA, 19146, USA

\*M. Akbari and F. Oghazian contributed equally to this work.

### **Abstract**

The authors of this research investigate the possibility of fabricating shell-based cellular structures using knitting techniques. Shellular Funicular Structures are two-manifold single-layer structures that can be designed in the context of graphic statics. These are efficient compression/tension-only structures that have been designed for a certain boundary condition. Although the shellular funicular structures are efficient geometries in transferring the forces, the fabrication process is challenging due to the geometric complexity of the structure. Since Shellular structures comprise a single surface, they are suitable candidates to be fabricated using knitting technique, a method by which yarn is manipulated to create a textile or fabric. Using knitting approach, one can fabricate shellular structures with minimum production waste in which the knit can work as a formwork for actual structure or act as a composite structure combined with bio-based resin. This research proposes a workflow to fabricate shellular structures using knitting that can be scaled up for industrial purposes. In this process, the designed shellular structures are divided into multiple sections that can be unrolled into planar geometries. These geometries are optimized based on the elastic forces in the knitted network and knitted and sewn to make a topologically complex geometry of the shellular systems. After assembling the knitted parts and applying external forces at the boundaries, the final configuration of the structural form in tension is achieved. Then this form is impregnated with custom bio-resin blends from chitosan, sodium alginate, and silk fibroin to stiffen the soft knit structures into a compressed system. Although this method is an efficient fabrication technique for constructing shellular structures, it needs to be translated into an optimized method of cutting, knitting, and sewing with respect to the complexity of the shellular geometry. As a proof of concept of the proposed workflow, a mesoscale shellular structure is fabricated.

**Keywords:** Biocomposite Structures, Shellular Funicular Structures, Knitting, Graphic statics.

#### 1. Introduction

The following section is divided into three primary sections. The initial section introduces a collection of spatial shell geometries known as shellular funicular structures, designed within the framework of graphic statics. The subsequent section discusses knitting structures and the historical progression of knitting techniques used in the development of shell structures. Lastly, the third section delves into





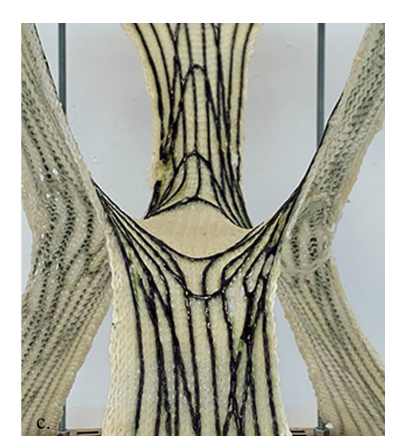


Figure 1: Biomaterial-based Stiffening of the knitting samples,

composite structures of fabric or knitting, which are subsequently solidified using synthetic or biological compunds.

#### 1.1. Shellular Funicular Structures

Shell structures are thin, curved plate structures that transfer forces through compression, tension, and shear stresses that act within the surface plane. These structures have numerous applications in science, design, and construction [1–3]. As a category of cellular structures, shell cellular (shellular) structures consist of continuous, smooth-curved shells. The geometry of these structures involves a surface with minimal material, known as a minimal surface [4]. The geometry of these surfaces, found in nature such as soap films, has inspired architects and engineers to design lightweight structures [5]. At each point on the minimal surface geometry, the mean curvature ( $H = k_1 \times k_2$ ) is zero, and the Gaussian curvature ( $G = k_1 \times k_2 < 0$ , considering  $k_1$  and  $k_2$  as the principal curvatures of the surface) is negative [6]. Due to their high surface-to-volume ratio and unique morphology, shells with these surfaces' geometry exhibit superior mechanical performance compared to other cellular structures, such as strut-based cellular structures [7–9].

Utilizing graphic statics as a method for structural design, designers can create structures using reciprocal diagrams while controlling the flow of force within the structure and the external loading scenario [10–14]. Polyhedral graphic statics (PGS), an extension of two-dimensional graphic statics (2DGS), enables the user to design axially-loaded structures in 3D, in which no bending occurs [15–17]. The form and force diagrams provide a clear relation between the geometry and the equilibrium of a 3-dimensional node (Figure 2a). In this technique, the form diagram (denoted by  $\Gamma$ ) represents the reaction forces combined with the geometry of the structure while each force diagram (denoted by  $\Gamma^{\dagger}$ ) explains the equilibrium of forces. Each strut member  $e_i$  in the form diagram is perpendicular to its corresponding face  $f_i^{\dagger}$  in the force diagram. In this technique, each vertex $v_i^{\dagger}$ , edge  $e_i^{\dagger}$ , face  $f_i^{\dagger}$ , and cell  $c_i^{\dagger}$  in the force diagram corresponds to a cell  $c_i$ , face  $f_i$ , edge  $e_i$ , and vertex  $v_i$  in the form diagram [15]. In this technique, the magnitude of the force in each strut member is proportional to the area of the corresponding face in the force diagram. By applying different subdivisions to a force diagram, various cellular strut-based structures in equilibrium can be designed (Figure 2a-d). Adding thickness to each edge of the form diagram proportional to the area of its corresponding face results in a strut-based cellular funicular structure.

The process of increasing the number of subdivisions in the force diagram leads to a form diagram with

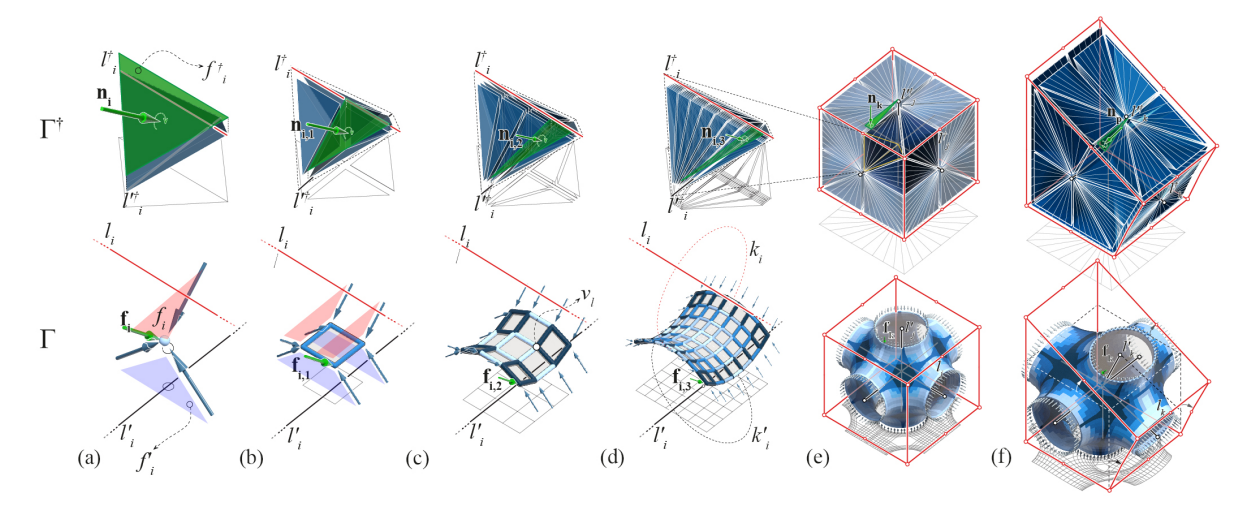


Figure 2: Iterative subdivision of a tetrahedron as a force diagram approximates a discrete surface with anticlastic curvature (a-d) as the form diagram. Using this subdivision between specific labyrinth graphs, one can design a shellular funicular structure (e) and use the labyrinths as control handles to manipulate the structure (f).

smaller edges and distributed forces in the members (Figure 2a-d). This procedure can eventually result in edges with near-zero length, approximating a surface as a form diagram. Polyhedral Graphic Statics (PGS) employs specific subdivision techniques to approximate surfaces with anticlastic or synclastic curvatures as form diagrams [9]. Figure 2a depicts a tetrahedron as a force diagram corresponding to a node in equilibrium with two upward and two downward forces as a form diagram (a node with an anticlastic curvature). This tetrahedron is produced by connecting the endpoints of the two skew lines  $l_i^{\mathsf{T}}$ and  $l_i^{\dagger}$ . Dividing these lines into equal segments and establishing a tetrahedron between every two skew segments from each line subdivides the force diagram into multiple tetrahedrons, resulting in a discrete anticlastic surface as a form diagram (Figure 2a-d) [9, 18]. This subdivision method is referred to as the anticlastic subdivision. These lines  $(l_i^{\dagger})$  and  $l_i^{\dagger}$  serve as subdivision axes in the force diagram and curvature axes in the form diagram (Figure 2d). These lines constitute two connectivity graphs known as labyrinths, which connect two segregated regions divided by the anticlastic surface in between [19]. By employing the anticlastic subdivision technique, one can design an anticlastic polyhedral surface, called a Shellular Funicular Structure (SFS) [20]. The labyrinths serve as subdivision axes in the form diagram and control handles in the force diagram, simplifying the design process and manipulation of the SFSs form-finding technique [18].

### 1.2. Knitted Structures

Historically, textiles have been a primary material used to develop fully tensioned structural systems. Knitted textiles, one of the many types of textiles, are created by producing loops with a continuous yarn and pulling that yarn through previously formed loops to create new ones. The resulting loops, or stitches, can be manipulated to form different stitch structures depending on the movement of the yarn. The structure of a knitted fabric is determined by the shaping of stitches, the manipulation of yarns, and the type of knitting machine used to create it. Knitted textiles have unique properties that make them suitable for developing complex and 3D shapes due to their multi-directional, heterogeneous and anisotropic characteristic [21]. Knitted textiles have been used in developing tension structures [22–25],

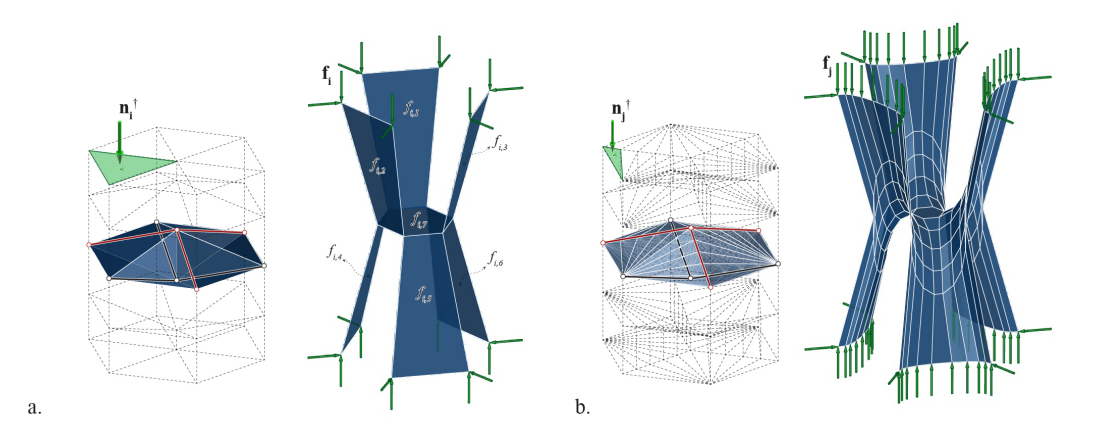


Figure 3: Designing a low-resolution (a) and high-resolution (b) of the force and form diagram of a shellular structure.

as well as in connection with concrete as a formwork system [26–28].

### 1.3. Biocomposite Structures

Materials such as silk, shell, chitin, cellulose, or bone present internal hierarchical configurations that confer stiffness, flexibility, and buckling resistance unmatched by man-made materials [29, 30]. Recent research in chemical and biomedical engineering has derived new synthesis methods to extract these materials from the natural structures they produce such as insect cocoons or shrimp shells [31, 32], and reverse-engineer them as water-based raw biopolymers to make new structures such as drug delivery micro-devices, tissue scaffolds, resolvable electronics, small object casts, and natural adhesives [33, 34] that are not only biocompatible to the human body but also able to be naturally decomposed. As in nature some of these materials perform as bio-resins binding together minerals and proteins into organism structures, we explore here if they could substitute toxic man-made synthetic resin compounds that are widely used as stiffeners of woven fiber structures (i.e epoxy, vinylester, or polyester resins used on carbon fiber, fiberglass, and aramid fiber). In this work, the authors used simple polysaccharides and proteins extracted from shrimp shells, algae cell walls, and silk cocoons, because of their biodegradability, strength, and flexibility properties, their compatibility with natural fibers of wool, cotton, and linen that compose our knits, and their proven ability to be precisely distributed in large additive manufacturing platforms as developed in the authors' previous work [35, 36].

### 1.4. Problem Statement and Objectives

Shellular funicular structures are highly efficient structures designed for a specific boundary condition. However, their fabrication process can be challenging due to their geometric complexity. Shellular structures, consisting of a single surface, are suitable for fabrication using the knitting technique, a process used to manipulate yarn to create fabric. Knitting can minimize production waste while serving as a formwork or composite structure, when combined with bio-based resin. This study proposes a workflow to fabricate shellular structures using knitting and scale them up for industrial purposes. The process involves dividing the designed shellular structures into sections that can be unrolled into planar geometries. These geometries are optimized based on the elastic forces in the knitted network and stitched together to form a topologically complex shellular system. After assembling the knitted parts, external forces are applied to achieve the final configuration of the structural form in tension. The form is then impregnated

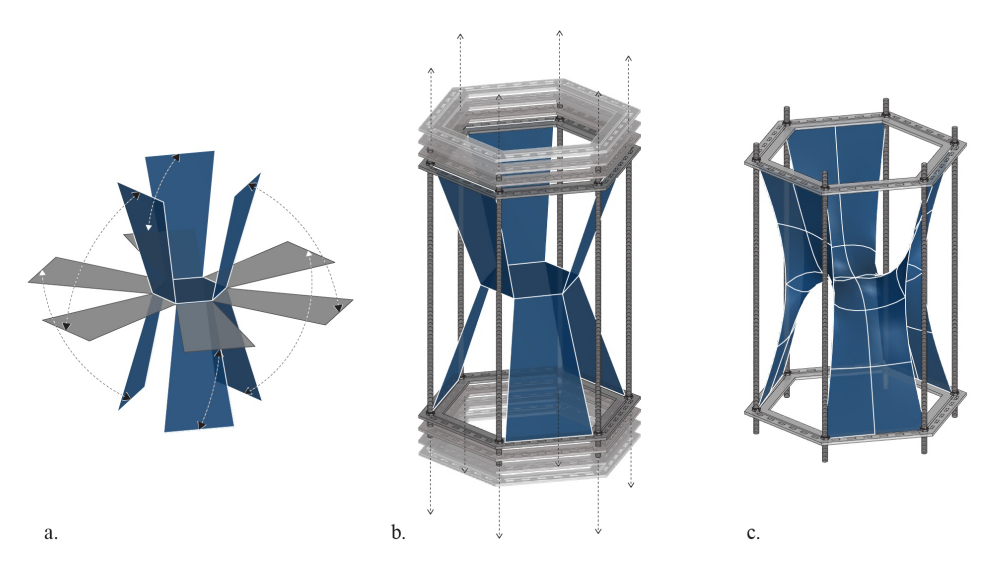


Figure 4: Unrolling the low-resolution shellular structure (a), and holding it using a jig (b). Turning the screws in the jig controls the height of the knit structure, assuring that the structure is in tension (c).

with custom bio-resin blends made from chitosan, sodium alginate, and silk fibroin to stiffen the soft knit structures into a compressed system. Although this method is efficient, an optimized method for cutting, knitting, and sewing must be developed to match the complexity of the shellular geometry. To demonstrate the proposed workflow's viability, a mesoscale shellular structure has been fabricated as a proof of concept.

# 2. Methodology

In this section, first, the process of designing a shallular structure for specific boundary conditions has been explained. In the next sections, this structure will be knitted and impregnated using bio-based materials. In the next section the knitting process will be explained through three different trials. In the last section, the biomaterial-based stiffening through different impregnation technique will be explained.

### 2.1. Shellular Structural Design

In order to develop a form for the structure in tension, shellular method in the context of graphic statics have been used [20, 37]. A rectangular prism (h:25 cm, w,l:20 cm) has been considered. Figure 3a displays the force diagram (left) corresponding to a structure comprising 30 edges, 7 faces, and 24 reaction forces. It is worth mentioning that the labyrinths graphs have been marked with black and red in the force diagram. Faces in the form diagram corresponding to these graphs have been removed in order to result in a 2-manifold structure [9]. To generate the form diagram, after designing the labyrinth graphs, a tetrahedron has been constructed for each pair of labyrinths (red and black labyrinths that are in a skew position together). This force diagram results in a low-resolution shellular funicular structure. The shellular structure with the higher resolution has a smoother surface along with a higher number of faces. In order to increase the smoothness of the structure, each labyrinth edge is subdivided into smaller segments, and a tetrahedron has been constructed between smaller edges in the force diagram (Figure 3b). In fact, each tetrahedron in Figure 3a is subdivided into 25 tetrahedrons in order to result in the force diagram in Figure 3b. This force diagram corresponds to a smooth form diagram, representing a shellular funicular structure.

In order to construct the geometry out of knitting, one needs to unroll the shellular structure to the XY plane. Due to the ease of unrolling the first form diagram prior to smoothing, the authors made the decision to unroll the form diagram consisting of seven faces. In this process, faces  $f_{i,1}$ ,  $f_{i,2}$ ,  $f_{i,3}$ ,  $f_{i,4}$ ,  $f_{i,5}$ ,  $f_{i,6}$  (Figure 3a), have been rotated along one of their edges in order to unroll the whole structure (Figure 4a). Using an elastic material for constructing this structure and tensioning it would result in a smooth structure, approximating the form diagram in Figure 3b. To apply tension to the structure, a jig comprising two flat panels and 6 screws have been constructed (Figure 4a). The screws will give the user the possibility to control the height of the structure, assuring that the whole knitting structure is in tension (Figure 4b).

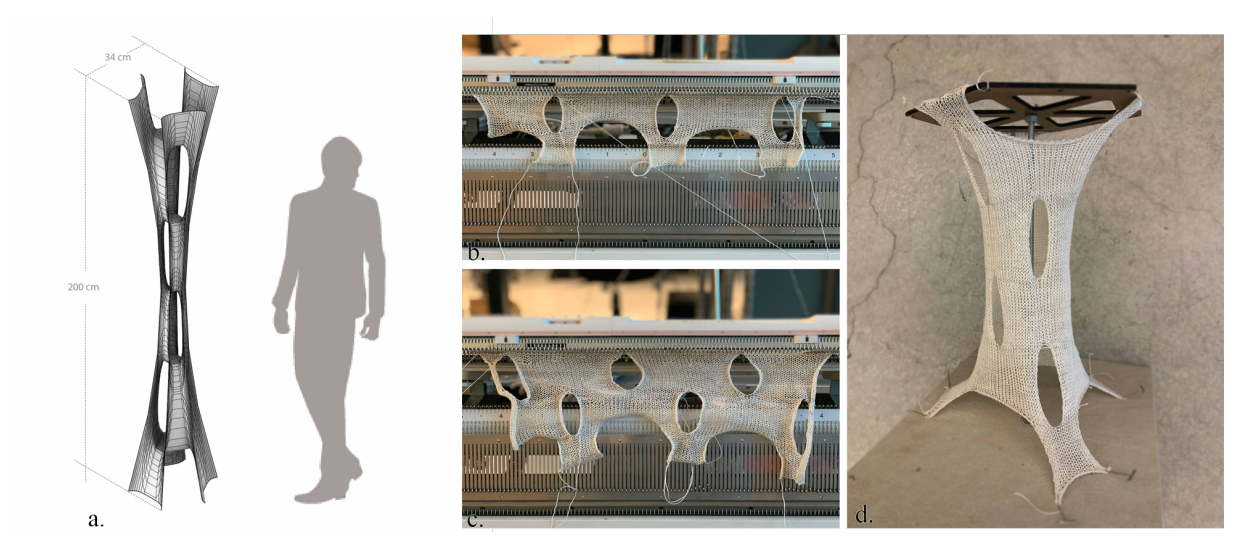


Figure 5: Trial 1, The geometry of a shellular funicular structure (a), the knitting fabrication of a shell (b,c), and the tensioned model of it (d).

# 2.2. Knitting Technology

The knitting process design for the shellular knit structure involves a series of trials aimed at achieving a seamless surface. The initial trial involved making a planar surface with holes, with the goal of making the entire surface seamless. However, the first attempt did not result in a shellular structure. For the second trial, a rough representation of the overall form was used, which was then unrolled as a seamless flat shape. The stitches were then generated over this flat shape and knitted. The knitted unrolled seamless flat shape was then sewn together to give an overall shape to the knitted textile. The rough 3D knitted structure was then tensioned to obtain a smooth tensioned structure. However, the model did not precisely replicate the digital model. Therefore, in the next step, efforts were made to increase the accuracy of the initial shape that should be knitted to achieve the final shape. At this stage, the focus was on only a portion of the overall form.

## 2.2.1. Trial 1

In the initial attempt, the focus was on creating a planar surface with holes (Figure 5). The aim of this trial was to knit the exterior skin first, and then add the interior planar surfaces. However, in this method, the exterior and interior surfaces were not connected and required more sewing to achieve the desired 3D shellular shape. This approach proved to be less efficient and required more effort and time to achieve the desired result. Therefore, further trials were conducted to explore alternative methods to create the

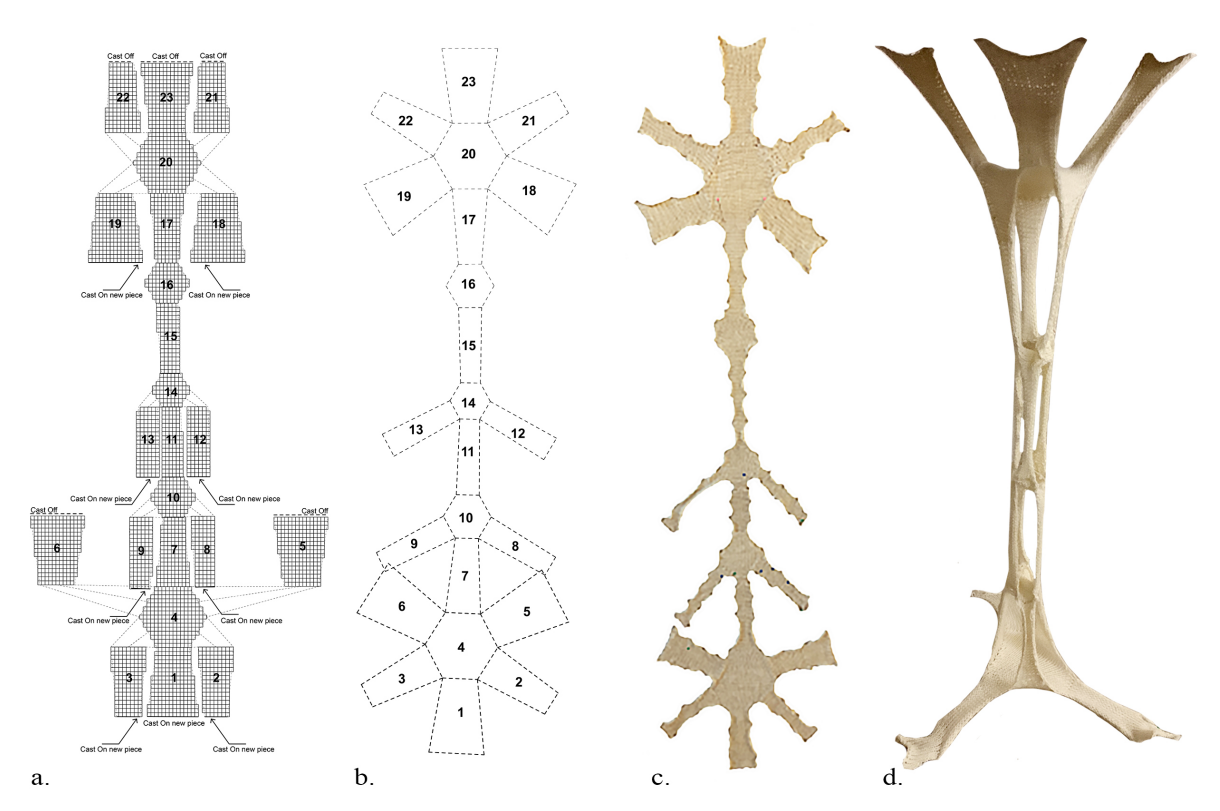


Figure 6: Trial 2, distribution of stitches (a), Sequence of knitting (b), knitted form pattern (c), the knitted structure in tension (d).

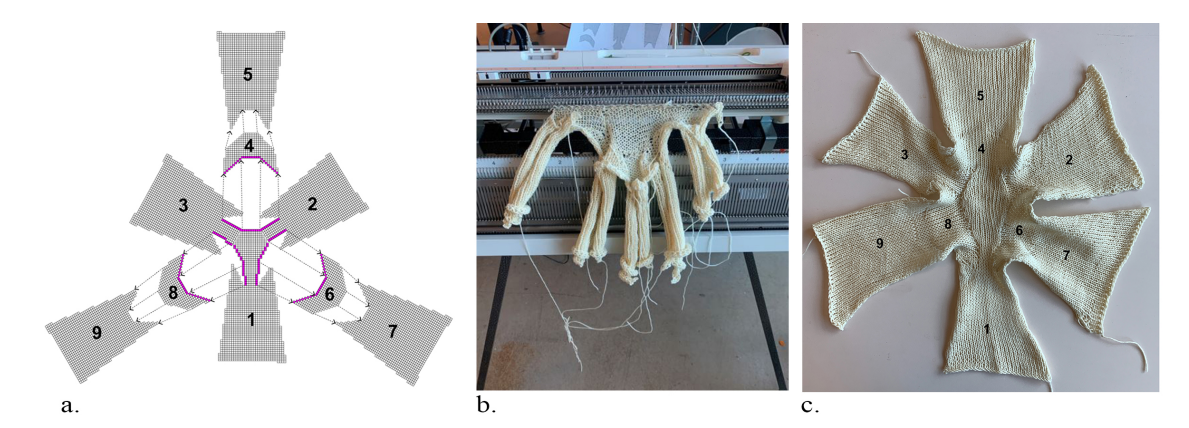


Figure 7: Trial 3, Sequence of knitting (a), Knitting fabrication (b), and Knitted piece for the main alternative (c).

shellular structure more efficiently and with fewer seams.

# 2.2.2. Trial 2

In the second trial, the authors aimed to improve the seamless feature of the shellular knit structure. To achieve this, the whole structure (Figure 5left) was unrolled and a single connection between the hexagons in the middle of the structure was ensured. The process involved creating a seamless flat shape

and generating the stitches over this flat shape. The objective was to create pieces with the knitting direction pointing towards the center of the hexagon. This was considered crucial as the direction of knitting plays a significant role in determining the behavior and performance of the textile. It was important to achieve a consistent behavior throughout the entire structure. Therefore, special attention was given to the direction of knitting during the fabrication process to ensure a more uniform and reliable behavior of the knitted textile. In addition, by ensuring a consistent knitting direction, the overall aesthetics of the structure were also improved, resulting in a more visually appealing end product. Figure 6 show the process of the knitting and after knitting the whole structure, in which the legs were sewn to the hexagon to obtain a rough 3D shape. This figure includes the unrolled diagram, distribution of the stitches, sequence of the knitting of different parts of the model, and the knit model in tension. By following this sequence, the authors were able to create a knitted shape that was more closely aligned with the digital model.

### 2.2.3. Trial 3

In order to achieve a higher degree of accuracy, the structure that is explained in section 2.1 is knitted. This structure is a portion of the structure displayed in Figure 5left, which is magnified in order to result in a more accurate model. The boundary shapes of this piece were then generated using a more precise digital model, and the stitches were generated accordingly. This approach aimed to improve the accuracy and consistency of the knitted structure, resulting in a more reliable and efficient end product.

### 2.3. Biomaterial-based Stiffening

Biomaterials used as bio-resins here are chitosan from shrimp shells, sodium alginate from algae cell walls, and Fibroin protein from silk cocoons. Silk Fibroin solution was produced by Canon Virginia Inc. Chitosan (medium molecular weight at 85% deacetylation) was purchased from TidalVision Inc. Acetic acid, glycerol, and sodium alginate were purchased from Sigma-Aldrich (USA). Fibroin aqueous solutions at 7%w/v combined with sodium alginate at 4.5%w/v as well as Chitosan at 4%w/v in 3%w/vacetic acid in gel solution are both blends used as homogeneous stiffeners throughout all knit samples (Figure 9). A blend of silk Fibroin at 7%w/v combined with sodium alginate at 4.5%w/v, natural coloring, and glycerol is used to additively manufacture targeted stiffening. To impregnate these blends onto knitted forms, casting and printing methods are used. Casting is based on spatula distribution of pre-measured biomaterial quantities according to surface area and knit thickness. Printing is performed with our exiting custom platform [35, 38]: a 3-axis computer numerically controlled (CNC) system with a 1x1m print bed that positions a pneumatic extrusion system in space. Toolpaths are designed in Rhinoceros3D® computer-aided design software and machine instructions are translated into custom Gcode via C# scripts. Positioning instructions are interpreted and sent via Serial Port JSON Server to the 3-axis CNC system. Extrusion machine instructions are sent via Serial Port to a dispense valve controller and precision valve using a 1.5mm inner diameter nozzle at 10PSI and receiving materials from 100PSI pressured reservoirs.

### 3. Results

The authors commenced their study by conducting experiments on stiffened knitted pieces composed of linen, wool, or cotton, as illustrated in Figure 8. Each of these materials was knitted in sparse and dense versions. The linen pieces were impregnated with Chitosan or Chitosan + Fibroin (Figure 8 S.01 - S.03). The wool pieces were impregnated with Fibroin + Alginate or Chitosan + Fibroin (Figure 8 S.04 - S.06). Lastly, the cotton pieces were impregnated with chitosan (Figure 8 S.07 - S.08). All specimens were subjected to loading after impregnation, and their loading capacity is presented in Figure 8. Based on the

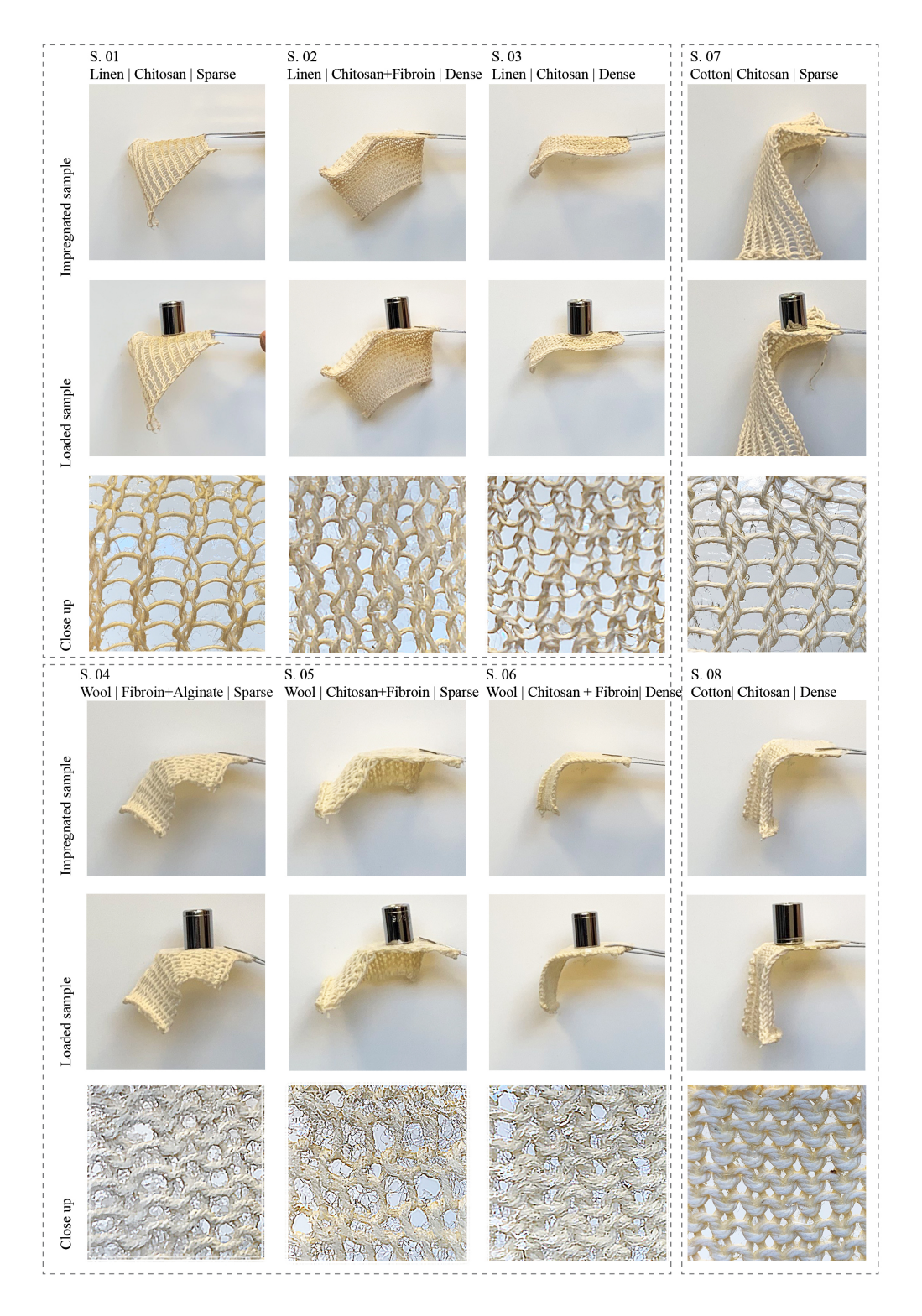


Figure 8: Biomaterial-based Stiffening of the knitting samples, in these experiments, only half of the knit is impregnated in order to compare the stiffness of the rigid part with the part that is draped.

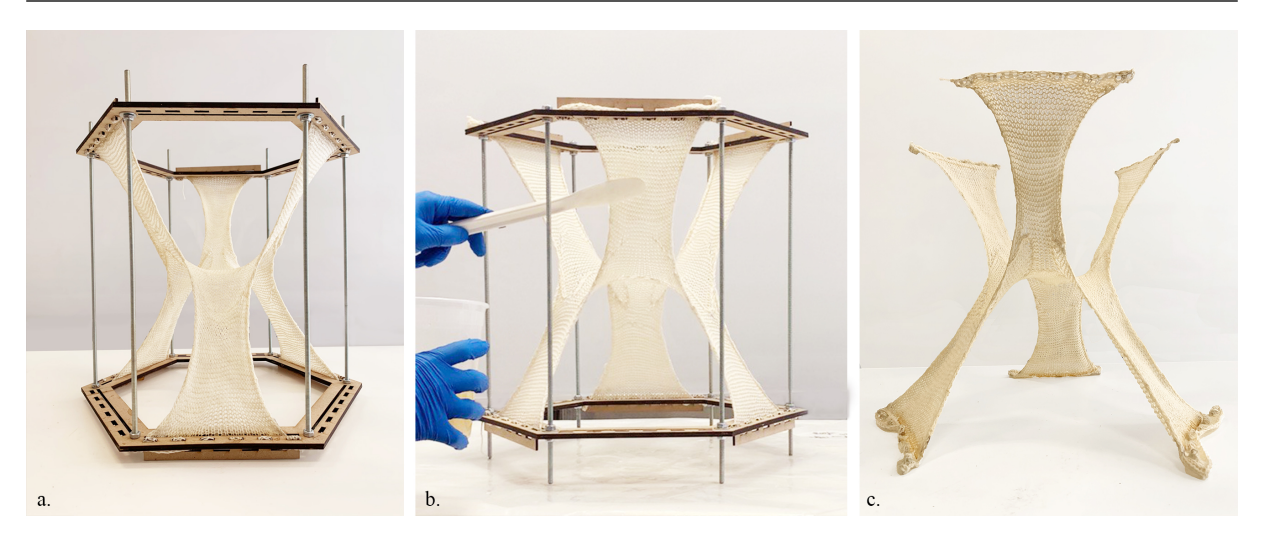


Figure 9: Biomaterial-based homogeneous stiffening of a knit structure: applying tension to the sample on the jig (a), impregnating the sample (b), and final structure after drying (c).



Figure 10: Biomaterial-based targeted stiffening; by impregnating the whole structure with a homogeneous Chitosan base layer (a), then printing a Fibroin-based stiffening toolpath on top (b), resulting in a fully impregnated piece with expected differential behavior (c).

experimental results, the primary knitted structure shown in Figure 7 was homogeneously stiffened by impregnating sparse wool knit with a blend of Chitosan + Fibroin (silk fibroin at 7%w/v combined with chitosan at 4%w/v) in the subsequent stage, and the model was held under tension in the jig. After one day, the dried model was loaded, and its structural capacity was evaluated. In the final stage, targeted heterogeneous stiffening was performed the same knitted model in Figure 7, a base impregnation of Chitosan (at 4%w/v) was followed by an additively manufactured layer of Fibroin + Alginate blend (using, in this case, silk fibroin at 7%w/v combined with sodium alginate at 4.5%w/v, natural coloring, and glycerol to optimize the blend for our printing technology). Given that the smooth version of the model in Figure 3a is depicted in Figure 3b, the pattern of the smooth model has been applied and projected onto the model prior to smoothing. In fact the pattern that is printed on the model displays the force flow of the smooth version of the model. This pattern would increase the material in places that we need, improving the structural capacity of the system. Figure 11 displays the process of global stiffening (with a clear Chitosan gel) and locally targeted stiffening of this specimen (with black silk fibroin blend).

In this process, a 3-axis computer numerically controlled (CNC) system with a 1x1m print bed has been used to print the pattern on top of the knitted piece. Final experimental results display that both global and local impregnation of the knitted structures results in a stiff structure with specific structural capacity. It is noteworthy that the structure depicted in Figures 7 requires an identical boundary condition to the one it has been designed for, to attain adequate structural capacity. Consequently, several tension ties are necessary at the top and bottom of the structure to reinforce it.

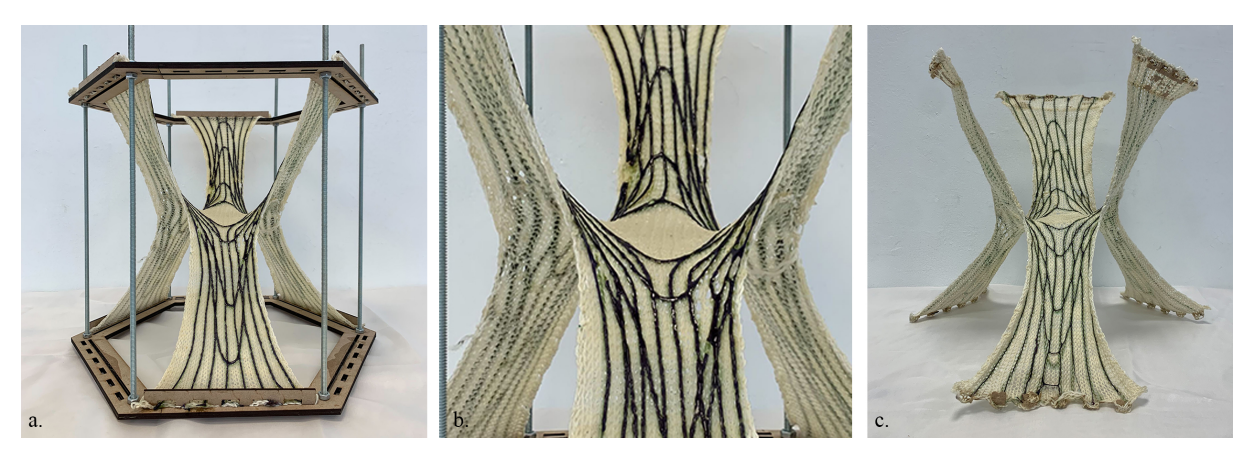


Figure 11: Biomaterial-based targeted stiffening.

### 4. Conclusion and Future Work

This research investigated the possibility of fabricating shell-based cellular structures using knitting techniques. The research proposed a workflow to fabricate shellular structures using knitting that can be scaled up for industrial purposes. In this process, the designed shellular structures are divided into multiple sections that can be unrolled into planar geometries. These geometries are optimized based on the elastic forces in the knitted network and knitted and sewn to make a topologically complex geometry of the shellular systems. After assembling the knitted parts and applying external forces at the boundaries, the final configuration of the structural form in tension is achieved. Then this form is impregnated with custom bio-resin blends from chitosan, sodium alginate, and silk fibroin to stiffen the soft-knit structures into a compressed system. In forthcoming research, it is crucial to concentrate on numerically assessing the structural efficacy of each structural specimen and contrasting it with experimental testing. Furthermore, it is imperative to concentrate on structures with greater dimensions, whose structural efficacy must be examined under actual loads.

### Acknowledgement

This research was partially funded by University Research Foundation (URF) to Dr. Laia Mogas-Soldevila. This research was also funded by the National Science Foundation CAREER Award (NSF CAREER-1944691 CMMI) and the National Science Foundation Future Eco Manufacturing Research Grant (NSF, FMRG-CMMI 2037097) to Dr. Masoud Akbarzadeh.

#### References

- [1] T. Teng, M. Jia, and J. E. Sabin, "The designing of epithelial cell inspired-brick inmasonry shell system," 2020.
- [2] T. Teng and J. Sabin, "The design and 4d printing of epithelial cell-inspired programmable surface geometry," 2021.
- [3] S. Adriaenssens, P. Block, D. Veenendaal, and C. Williams, *Shell structures for architecture: form finding and optimization*. Routledge, 2014.
- [4] W. Meeks III and J. Pérez, "The classical theory of minimal surfaces," *Bulletin of the American Mathematical Society*, vol. 48, no. 3, pp. 325–407, 2011.
- [5] B. Burkhardt, "Natural structures-the research of frei otto in natural sciences," *International journal of space structures*, vol. 31, no. 1, pp. 9–15, 2016.
- [6] D. Hilbert and S. Cohn-Vossen, *Geometry and the Imagination*, vol. 87. American Mathematical Soc., 2021.
- [7] S. C. Han, J. W. Lee, and K. Kang, "A new type of low density material: Shellular," *Advanced Materials*, vol. 27, no. 37, pp. 5506–5511, 2015.
- [8] S. C. Han, J. M. Choi, G. Liu, and K. Kang, "A microscopic shell structure with schwarz's d-surface," *Scientific reports*, vol. 7, no. 1, pp. 1–8, 2017.
- [9] M. AKBARI, M. AKBARZADEH, and M. BOLHASSANI, "From polyhedral to anticlastic funicular spatial structures," in *Proceedings of IASS Symposium*, 2019.
- [10] J. C. Maxwell, "On Reciprocal Figures and Diagrams of Forces," *Philosophical Magazine Series 4*, vol. 27, no. 182, pp. 250–261, 1864.
- [11] W. J. M. Rankine, "Principle of the Equilibrium of Polyhedral Frames," *Philosophical Magazine Series 4*, vol. 27, no. 180, p. 92, 1864.
- [12] L. L. Beghini, J. Carrion, A. Beghini, A. Mazurek, and W. F. Baker, "Structural Optimization Using Graphic Statics," *Structural and Multidisciplinary Optimization*, vol. 49, no. 3, pp. 351–366, 2013.
- [13] L. Cremona, *Graphical Statics: Two Treatises on the Graphical Calculus and Reciprocal Figures in Graphical Statics. Translated by Thomas Hudson Beare*. Oxford: Clarendon Press, 1890.
- [14] K. Culmann, Die Graphische Statik. Zürich: Verlag Meyer und Zeller, 1864.
- [15] M. Akbarzadeh, *3D Graphic Statics Using Reciprocal Polyhedral Diagrams*. PhD thesis, ETH Zurich, Zurich, Switzerland, 2016.
- [16] Y. Lu, M. Cregan, P. Chhadeh, A. Seyedahmadian, M. Bolhassani, J. Schneider, J. Yost, and M. Akbarzadeh, "All glass, compression-dominant polyhedral bridge prototype: form-finding and fabrication," in *Proceedings of IASS Symposium and Spatial Structures Conference 2020/21, Inspiring the next generation*, (Guildford, UK), August 23-27 2021.
- [17] H. Chai and M. Akbarzadeh, "Web-based Interactive Polyhedral Graphics Statics Platform," in *Proceedings of the IASS Annual Symposium 2020/21*, (Surrey,UK), 2021.

- [18] M. Akbari, A. Mirabolghasemi, H. Akbarzadeh, and M. Akbarzadeh, "Geometry-based structural form-finding to design architected cellular solids," in *Symposium on Computational Fabrication*, pp. 1–11, 2020.
- [19] W. Fischer and E. Koch, "Genera of minimal balance surfaces," *Acta Crystallographica Section A: Foundations of Crystallography*, vol. 45, no. 10, pp. 726–732, 1989.
- [20] M. Akbari, A. Mirabolghasemi, M. Bolhassani, A. Akbarzadeh, and M. Akbarzadeh, "Strut-based cellular to shellular funicular materials," *Advanced Functional Materials*, p. 2109725, 2022.
- [21] C. L. McKnelly, *Knitting behavior: a material-centric design process*. PhD thesis, Massachusetts Institute of Technology, 2015.
- [22] R. La Magna, V. Fragkia, R. Noël, Y. Šinke, M. Tamke, P. Längst, J. Lienhard, and M. Thomsen, "Isoropia: an encompassing approach for the design, analysis and form-finding of bending-active textile hybrids," 07 2018.
- [23] M. R. Thomsen, M. Tamke, A. Karmon, J. Underwood, C. Gengnagel, N. Stranghöner, and J. Uhlemann, "Knit as bespoke material practice for architecture," in *Acadia 2016*, pp. 280–289, ACADIA, 2016.
- [24] J. E. Sabin, "mythread pavilion: generative fabrication in knitting processes," in *ACADIA*, vol. 13, pp. 347–354, 2013.
- [25] J. E. Sabin, J. Hilla, D. Pranger, C. Binkley, and J. Bilotti, "Embedded architecture: Ada, driven by humans, powered by ai," *Fabricate 2020*, pp. 246–255, 2020.
- [26] A. Pal, W. L. Chan, Y. Y. Tan, P. Z. Chia, and K. J. Tracy, "Knit concrete formwork," in *Proceedings of the 25th CAADRIA Conference*, vol. 1, pp. 213–22, 2020.
- [27] M. Popescu, L. Reiter, A. Liew, T. Van Mele, R. J. Flatt, and P. Block, "Building in concrete with an ultra-lightweight knitted stay-in-place formwork: prototype of a concrete shell bridge," in *Structures*, vol. 14, pp. 322–332, Elsevier, 2018.
- [28] M. Popescu, M. Rippmann, A. Liew, L. Reiter, R. J. Flatt, T. Van Mele, and P. Block, "Structural design, digital fabrication and construction of the cable-net and knitted formwork of the knitcandela concrete shell," in *Structures*, vol. 31, pp. 1287–1299, Elsevier, 2021.
- [29] J. Vincent, Structural biomaterials. Princeton University Press, 2012.
- [30] M. A. Meyers, J. Mckittrick, and P.-Y. Chen, "Structural Biological Materials: Critical Mechanics-Materials Connections," *Science*, vol. 335, pp. 199–204, jan 2012.
- [31] J. G. Fernandez and D. E. Ingber, "Bioinspired chitinous material solutions for environmental sustainability and medicine," *Advanced Functional Materials*, vol. 23, no. 36, pp. 4454–4466, 2013.
- [32] F. G. Omenetto and D. L. Kaplan, "New opportunities for an ancient material.," *Science (New York, N.Y.)*, vol. 329, no. 5991, pp. 528–531, 2010.
- [33] G. Guidetti, L. D'Amone, T. Kim, G. Matzeu, L. Mogas-Soldevila, B. Napier, N. Ostrovsky-Snider, J. Roshko, E. Ruggeri, and F. G. Omenetto, "Silk materials at the convergence of science, sustainability, healthcare, and technology," *Applied Physics Reviews*, vol. 9, p. 011302, mar 2022.

- [34] J. G. Fernandez and D. E. Ingber, "Manufacturing of large-scale functional objects using biodegradable chitosan bioplastic," *Macromolecular Materials and Engineering*, vol. 299, no. 8, 2014.
- [35] L. Mogas-Soldevila, G. Matzeu, M. L. Presti, and F. Omenetto, "Additively manufactured leather-like silk protein materials," *Materials Design*, vol. 203, p. 109631, 2021.
- [36] L. Mogas-Soldevila, J. Duro-Royo, and N. Oxman, "Water-Based Robotic Fabrication: Large-Scale Additive Manufacturing of Functionally Graded Hydrogel Composites via Multichamber Extrusion," 3D Printing and Additive Manufacturing, vol. 1, pp. 141–151, sep 2014.
- [37] M. Akbari and M. Akbarzadeh, "Continuous approximation of shellular funicular structures," in *Proceedings of IASS 2022 symposium affiliated with APCS 2022 conference*, (Beijing, China), September 19-22 2022.
- [38] G. Ho, V. Kubušová, C. Irabien, V. Li, A. Weinstein, S. Chawla, D. Yeung, A. Mershin, K. Zolotovsky, and L. Mogas-Soldevila, "Multiscale design of cell-free biologically active architectural structures," *Frontiers in Bioengineering and Biotechnology*, vol. 11, 2023.